Order and frustration in chiral liquid crystals

2001 J. Phys.: Condens. Matter 13 R1

(http://iopscience.iop.org/0953-8984/13/3/201)

INSTITUTE OF PHYSICS PUBLISHING JOURNAL OF PHYSICS: CONDENSED MATTER

J. Phys.: Condens. Matter **13** (2001) R1–R22 www.iop.org/Journals/cm PII: S0953-8984(01)08651-9

TOPICAL REVIEW

Order and frustration in chiral liquid crystals

Randall D Kamien[1] **and Jonathan V Selinger**[2]

[1] Department of Physics and Astronomy, University of Pennsylvania, Philadelphia, PA 19104, USA
[2] Center for Bio/Molecular Science and Engineering, Naval Research Laboratory, Code 6900, Washington, DC 20375, USA

Received 11 September 2000, in final form 28 November 2000

Abstract

This article reviews the complex ordered structures induced by chirality in liquid crystals. In general, chirality favours a twist in the orientation of liquid-crystal molecules. In some cases, as in the cholesteric phase, this favoured twist can be achieved without any defects. More often, the favoured twist competes with applied electric or magnetic fields or with geometric constraints, leading to frustration. In response to this frustration, the system develops ordered structures with periodic arrays of defects. The simplest example of such a structure is the lattice of domains and domain walls in a cholesteric phase under a magnetic field. More complex examples include defect structures formed in two-dimensional films of chiral liquid crystals. The same considerations of chirality and defects apply to three-dimensional structures, such as the twist-grain-boundary and moiré phases.

(Some figures in this article are in colour only in the electronic version; see `www.iop.org`)

1. Introduction

Frustration is the competition between different influences on a physical system that favour incompatible ground states. The phenomenon of frustration has been studied in a wide range of systems because it makes nature interesting: under competing influences, a system can develop structures with complex spatial organization, and can have a rich variety of transitions between different ordered phases.

A prototypical example of frustration on a lattice is an Ising antiferromagnet. On a periodic, one-dimensional lattice with an *odd* number of sites N, the system cannot have a perfect alternation in the spin, and hence it must have one frustrated bond. As a result, there are $2N$ degenerate ground states corresponding to the number of locations for the frustrated bond. The situation becomes more complicated on a two-dimensional triangular lattice, in which frustration leads to complex ordered structures with dimerization of the spins [1]. If there were no frustration between the geometry and the interactions, the rich phase diagram of these simple lattice systems would disappear.

Frustration can also occur in continuum systems. For example, a superconductor in a magnetic field either expels magnetic field in the superconducting phase or becomes a normal

metal and allows magnetic flux into the bulk. The Abrikosov vortex is the compromise that balances these frustrated extremes. While the normal metal and the superconducting phases are translationally invariant, the Abrikosov phase of a type-II superconductor is a flux-line lattice, which creates a new level of organization at a new length scale set by the flux-line interactions and the applied magnetic field [2].

In this review, we discuss the frustration that occurs in the liquid-crystalline phases of *chiral* molecules. A molecule is chiral if it cannot be superimposed on its mirror image via any proper rotation or translation. Since the birth of stereochemistry in 1848 with Pasteur's discovery of molecular handedness [3], the role of chirality has become ever more important. Pharmaceuticals, food additives, electro-optic devices, and liquid-crystal displays are examples of technologies that use or rely on the effect of chiral constituents.

In the context of liquid crystals, the main effect of chirality is that chiral molecules do not tend to pack parallel to their neighbours, but rather at a slight skew angle with respect to their neighbours. This packing can be visualized, for example, by the packing of hard screws, although the details of the chiral interaction are somewhat more subtle [4, 5]. As a result, chirality favours a macroscopic twist in the orientation of the molecules, with a characteristic chiral length scale. This favoured twist leads to the self-assembly of periodically ordered structures. Recently, these self-assembling structures have been used as templates [6] in the nano- and micro-fabrication of a host of technologically interesting materials [7, 8], often with remarkable electro-optic properties. Thus, the prediction, characterization, and control of self-assembling structures is likely to be an essential ingredient in the quest for ever more useful and economical devices.

In some cases, the twist in the molecular orientation favoured by chirality can be achieved without the introduction of any defects. Two common examples of such defect-free structures are the cholesteric phase and the helically twisted smectic-C* phase. More often, however, the twist favoured by chirality competes with other influences on a liquid-crystal system, such as applied magnetic or electric fields or constraints imposed by geometry. In those situations, the competition leads to frustration, which causes the liquid crystal to develop complex ordered structures. Such structures are the subject of this paper.

The plan of this paper is as follows.

We begin with a cholesteric liquid crystal in an applied magnetic field. This example serves as a tutorial in frustration because the mathematics is straightforward and can be solved exactly. The system is frustrated because of the competition between chirality, which favours a twist in the molecular orientation, and the magnetic field, which favours alignment of the molecules. This frustration leads to the formation of a series of domains in which the molecules are approximately aligned with the field, separated by domain walls, or solitons, in which the molecular orientation twists rapidly.

In the next section, we consider defect structures that form in two-dimensional films of liquid crystals. These films have a different type of frustration, which is not imposed by an applied field but is intrinsic to the two-dimensional geometry: chirality favours a modulation in the molecular orientation, but this modulation cannot be achieved in two dimensions without the introduction of defects, i.e. solitons in the molecular orientation. We discuss the ordered defect lattices that can arise, as well as variations in the structures involving chiral symmetry breaking and curvature in the film.

Finally, we consider defect structures in three-dimensional liquid-crystal systems. These structures include the twist-grain-boundary (TGB) phase, which arises from the frustration of chirality combined with a smectic density wave. Although these structures are much more complex than the cholesteric and two-dimensional examples, they arise from the same considerations of order, frustration, and defects.

2. The cholesteric in a magnetic field: a tutorial example of frustration

As an example of how chirality can frustrate liquid-crystalline order, we will review the classic work of Meyer describing a cholesteric phase in a magnetic field [9]. In this system, frustration arises from the competition between chirality, which favours a twist in the molecular orientation, and the applied magnetic field, which favours alignment of the molecules along the field. We will show that the system balances these opposing influences by introducing domain walls—one-dimensional analogues of Abrikosov vortices. Indeed, domain walls and Abrikosov vortices can be regarded as different types of solitons.

A cholesteric phase is described by the local director $\hat{\boldsymbol{n}}$, a unit vector that points along the average molecular direction. The free energy of spatial distortions in the director under a uniform magnetic field $\boldsymbol{H}$ is given by the Frank free energy [10]

$$F = \frac{1}{2}\int \mathrm{d}^3x \, \{K_1[\boldsymbol{\nabla}\cdot\hat{\boldsymbol{n}}]^2 + K_2[\hat{\boldsymbol{n}}\cdot\boldsymbol{\nabla}\times\hat{\boldsymbol{n}} + q_0]^2 + K_3[\hat{\boldsymbol{n}}\times(\boldsymbol{\nabla}\times\hat{\boldsymbol{n}})]^2 - \chi_M[\boldsymbol{H}\cdot\hat{\boldsymbol{n}}]^2\} \tag{1}$$

where K_1, K_2, and K_3 are elastic constants describing splay, twist, and bend, respectively, $2\pi/q_0$ is the cholesteric pitch and χ_M is the anisotropy of the magnetic susceptibility of the nematic (which we will take to be positive).

If the chiral parameter $q_0 = 0$, the system has a simple *uniform* ground state. In this case, the director $\hat{\boldsymbol{n}}$ is aligned with the magnetic field $\boldsymbol{H}$, with no spatial variation. By comparison, if the field $\boldsymbol{H} = 0$, the system has a simple *twisted* ground state, with the continuously twisting, defect-free cholesteric texture $\hat{\boldsymbol{n}} = [0, \cos(q_0x), \sin(q_0x)]$. (This solution can, of course, be rotated so that the pitch axis points in an arbitrary direction.) The question is now: what happens if both q_0 and $\boldsymbol{H}$ are nonzero?

The simplest, approximate way to answer this question is to compare the free energies of the uniform and twisted states. The free-energy density of the uniform state in the presence of nonzero q_0 is $\mathcal{F}_{\mathrm{uni}} = \frac{1}{2}K_2[q_0^2 - \xi^{-2}]$, where $\xi^{-2} \equiv \chi_M H^2/K_2$. The free-energy density of the twisted state in the presence of nonzero $\boldsymbol{H}$, perpendicular to the pitch axis, is $\mathcal{F}_{\mathrm{twist}} = -\frac{1}{4}K_2\xi^{-2}$. We can compare these free-energy densities to estimate the critical value of q_0 at which one state is favoured over the other: we expect the twisted state whenever $q_0 \geqslant 1/(\sqrt{2}\xi)$. However, this is only an approximation because the system has many degrees of freedom and it can compromise between the uniform and twisted states. We will see that this estimate is close but not correct.

For an exact solution, we consider a cholesteric phase with the helical axis along the x-axis in a uniform magnetic field along the z-axis. The director depends on the angle $\theta(x)$: $\hat{\boldsymbol{n}} = [0, \cos\theta(x), \sin\theta(x)]$. The full free energy is

$$\frac{F}{A} = \frac{1}{2}\int \mathrm{d}x \, \left\{K_2\left[\frac{\mathrm{d}\theta(x)}{\mathrm{d}x} - q_0\right]^2 - \chi_M H^2 \sin^2\theta(x)\right\} \tag{2}$$

where we have divided out the yz cross-sectional area A. We recognize this free energy as the classic sine–Gordon model [11]. It can be rewritten as the sum

$$\frac{F}{A} = \frac{1}{2}K_2\int \mathrm{d}x \, \left\{\left[\left(\frac{\mathrm{d}\theta}{\mathrm{d}x}\right)^2 + \xi^{-2}\cos^2\theta\right] - 2q_0\frac{\mathrm{d}\theta}{\mathrm{d}x} + q_0^2\right\}. \tag{3}$$

This decomposition enables us to study the effect of q_0 for fixed field. The first pair of terms (in square brackets) favours uniform domains with $\theta = (m + \frac{1}{2})\pi$, for any integer m, which all represent alignment of the director along $\boldsymbol{H}$. The next term favours an increase of $\theta(x)$ from one domain to the next, giving a domain wall or soliton. (The final term is an unimportant

constant.) When q_0 becomes sufficiently large, the system gains more free energy from a domain wall (from the $\mathrm{d}\theta/\mathrm{d}x$ term) than it loses (from the first pair of terms), and hence a single domain wall forms. As q_0 is increased above this threshold value, more domain walls form, giving a periodic lattice of alternating domains and domain walls, as shown in figure 1. In the limit of high q_0, the density of domain walls increases and the system approaches the continuously twisting cholesteric state.

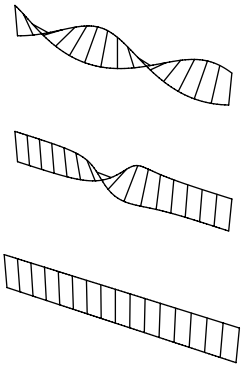

Figure 1. A cholesteric helix under an applied magnetic field. Top: a continuously twisting helix, in the limit of $q_0 \gg 2/(\pi\xi)$. Middle: a single domain wall between two uniform domains, for $q_0 \gtrsim 2/(\pi\xi)$. Bottom: a uniform state, for $q_0 < 2/(\pi\xi)$.

To find the threshold at which the first domain wall forms, the standard approach is to minimize the free energy of equation (3) by solving the corresponding Euler–Lagrange equation [12]. Here, we will follow an alternative approach, employing the method of Bogomol'nyi [13], which simplifies the calculation. To do this, we rewrite equation (3) as

$$\frac{F}{A} = \frac{1}{2}K_2 \int \mathrm{d}x \left\{ \left[\frac{\mathrm{d}\theta}{\mathrm{d}x} - \xi^{-1}\cos\theta \right]^2 - 2\,\frac{\mathrm{d}}{\mathrm{d}x}\left[q_0\theta - \xi^{-1}\sin\theta \right] + \left[q_0^2 - \xi^{-2} \right] \right\}. \tag{4}$$

The first term of this expression is positive-definite, and it vanishes if

$$\frac{\mathrm{d}\theta}{\mathrm{d}x} = \xi^{-1}\cos\theta. \tag{5}$$

This differential equation has solutions corresponding to a uniform state ($\theta = \pm\pi/2$) and to a single domain wall ($\theta(x) = \pi/2 - 2\tan^{-1}[\exp(-(x - x_{\mathrm{wall}})/\xi)]$), and hence the first term vanishes for both cases. The difference in free energies between these states therefore comes only from the second term—a total derivative which integrates to the boundaries at infinity and hence only depends on the topological winding of the solution. In the uniform state, $\theta(x)$ is the same at $\pm\infty$, but if there is a single domain wall, then $\theta(x)$ changes from $-\pi/2$ to $\pi/2$. Hence, the free energy of a single domain wall, compared with the free energy of the uniform state, is

$$\frac{F_{\mathrm{wall}} - F_{\mathrm{uni}}}{A} = K_2(2\xi^{-1} - \pi q_0). \tag{6}$$

Thus, the single domain wall is favoured for $q_0 \geqslant 2/(\pi\xi)$, close to but smaller than our earlier estimate $q_0 \geqslant 1/(\sqrt{2}\xi)$.

This example shows that a uniform ground state pointing along the magnetic field is incompatible with chirality. The frustration is resolved through the introduction of a domain wall, or soliton, which takes the system from one domain to another, equivalent domain. In the

following sections we will describe higher-dimensional systems that share this feature—the frustrating effect of chirality will be relieved through solitons that connect equivalent domains. Although the mathematics will become more complex, the essential idea will be the same. In some cases these solitons will be *topological defects* [14], although we will not be focusing on that aspect in this review.

3. Defect structures in two dimensions

3.1. Geometric frustration

In section 2, we showed how an aligning magnetic field can be frustrated by chiral interactions in materials. This type of frustration is somewhat artificial since the magnetic field is externally applied. However, geometry often plays a role similar to an external field—boundary conditions in a finite-sized sample often compete with the intrinsic interactions [15, 16]. Similarly, when liquid crystals are confined between two plates [17], in a capillary [18, 19], or in a droplet [20], the shape of the sample can alter the bulk ground-state structures.

Geometric effects are even more profound in two-dimensional systems. When liquid crystals are confined to two dimensions, the system cannot have a defect-free chiral modulation, as in a three-dimensional cholesteric phase in zero magnetic field. Rather, the system can only express structural chirality by introducing defects, i.e. solitons.

This geometric frustration can be seen graphically in figure 2. This figure shows a two-dimensional film of liquid crystals in a smectic-C or other tilted phase. The arrows represent the projection $\boldsymbol{c}(x, y)$ of the three-dimensional molecular director $\hat{\boldsymbol{n}}(x, y)$ into the smectic layer plane. If the system were to have a defect-free chiral modulation, analogous to a three-dimensional cholesteric phase, then $\boldsymbol{c}$ would have to rotate through an angle of 2π as a function of x, as shown in the figure. Is such a structure favoured by chirality? Note that this structure can be divided into alternating regions labelled 1 and 2. These two regions are actually *mirror images* of each other. For that reason, they cannot both be favoured by chirality. If one is favoured, then the other is disfavoured to exactly the same extent. Hence, this structure will not occur in a two-dimensional film of chiral liquid crystals. Instead, the film must have regions with the favoured modulation in $\boldsymbol{c}$ (either 1 or 2, depending on the handedness of the material), separated by defect walls, in which $\boldsymbol{c}$ jumps back so that it can have the favoured modulation once again.

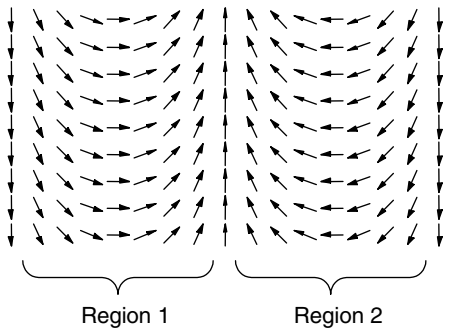

Figure 2. Hypothetical defect-free modulation in a two-dimensional film of liquid crystals in a smectic-C or other tilted phase. The arrows represent the projection of the three-dimensional molecular director into the smectic layer plane. Note that regions 1 and 2 are mirror images of each other, with opposite signs of the bend in the director. Hence, this structure is *not* favoured by chirality.

The same geometric frustration can also be understood mathematically. Again consider a two-dimensional film of liquid crystals in the smectic-C phase. If the magnitude of the molecular tilt is uniform, with the result that the projection $\boldsymbol{c}$ has constant length, then the only chiral term in the bulk free energy is

$$F_{\text{chiral}} = \int \mathrm{d}^2x \; [-\lambda \hat{\boldsymbol{z}} \cdot \boldsymbol{\nabla} \times \boldsymbol{c}] \tag{7}$$

which favours bend in $\boldsymbol{c}$. This term is a total derivative, which can be reduced to a line integral around the edges of the liquid-crystal domain. Moreover, if the modulation is in the x-direction, as in figure 2, the chiral term simplifies to

$$F_{\text{chiral}} = \int \mathrm{d}^2x \; \left[-\lambda \frac{\partial c_y}{\partial x}\right] \tag{8}$$

and the corresponding line integral is just

$$F_{\text{chiral}} = -\lambda L[c_y(x_{\max}) - c_y(x_{\min})] \tag{9}$$

where L is the system size in the y-direction. This expression for the chiral term shows explicitly that chirality favours an increase in c_y across the width of a domain, from $x_{\min}$ to $x_{\max}$. The magnitude of this increase is limited, because c_y can at most increase from -1 to $+1$. Hence, if the system had only a single domain, it could have at most a chiral free energy of $F_{\text{chiral}} = -2\lambda L$, which does not even scale with the system size in the x-direction. The only way for the system to have a more favourable chiral free energy is to break up into finite domains separated by domain walls, giving a chiral contribution of roughly $-2\lambda L$ for *each domain*. This tendency to form domain walls, which can also be regarded as defect lines or solitons, is an expression of geometric frustration.

As an aside, we note that a similar type of geometric frustration occurs in two-dimensional films with an *up–down* asymmetry rather than a chiral asymmetry. Such systems include Langmuir monolayers, Langmuir–Blodgett films, and surface layers in liquid crystals. In pioneering experimental and theoretical work, Meyer and Pershan showed that the up–down asymmetry favours a splay in $\boldsymbol{c}$ [21]. This is analogous to the bend favoured by chirality, if $\boldsymbol{c}$ is rotated by 90°, transforming bend into splay. Hence, the results of the following sections apply also to films with up–down asymmetry, with this rotation in $\boldsymbol{c}$.

3.2. Lattice of defect lines

We have argued in the previous section that two-dimensional films of chiral liquid crystals have a geometric frustration, which leads them to break up into domains separated by defect lines. For that reason, one would expect such films to show a lattice of defect lines. Such a defect lattice has been observed in polarization micrographs of freely suspended thin films [22, 23], and related but more complex lattices have been seen in thicker films [24]. The defect lattice has been studied theoretically by several authors [25–28]. In this and the following section, we discuss the theory of the defect lattice, combining the theoretical approaches of those authors.

For the simplest and most macroscopic theory, we can regard the liquid-crystal film as a sequence of alternating domains and domain walls. In this view, the domains can be described by continuum elastic theory, while the domain walls are just defect lines with some phenomenological energy ϵ per unit length. For the domains, the free energy is just the chiral term discussed in the previous section plus the two-dimensional Frank free energy,

$$F = \int \mathrm{d}^2x \left[-\lambda \hat{\boldsymbol{z}} \cdot \boldsymbol{\nabla} \times \boldsymbol{c} + \frac{1}{2}K_1(\boldsymbol{\nabla} \cdot \boldsymbol{c})^2 + \frac{1}{2}K_3(\hat{\boldsymbol{z}} \cdot \boldsymbol{\nabla} \times \boldsymbol{c})^2\right]. \tag{10}$$

A precise minimization of this free energy was discussed in reference [25]. However, the most important features of the results can be seen in the following approximate calculation. Suppose that the system has a striped pattern as shown in figure 3, with a stripe width of d. Across each stripe, $\boldsymbol{c}$ rotates through an angle of order π, which gives

$$\boldsymbol{\nabla} \cdot \boldsymbol{c} \approx \hat{\boldsymbol{z}} \cdot \boldsymbol{\nabla} \times \boldsymbol{c} \approx \frac{1}{d}. \tag{11}$$

Inserting these approximations into equation (10) gives the free energy of a single stripe:

$$F_{\text{stripe}} = dL\left[-\frac{\lambda}{d} + \frac{\bar{K}}{d^2}\right] \tag{12}$$

where $\bar{K} = \frac{1}{2}(K_1 + K_3)$ is the mean Frank constant. To this expression must be added the free energy of a single domain wall:

$$F_{\text{wall}} = L\epsilon. \tag{13}$$

Combining these terms gives the free energy per unit area:

$$\frac{F}{A} = \frac{F_{\text{stripe}} + F_{\text{wall}}}{dL} = -\frac{\lambda - \epsilon}{d} + \frac{\bar{K}}{d^2}. \tag{14}$$

Minimizing this free-energy density over d gives the stripe width

$$d = \frac{2\bar{K}}{\lambda - \epsilon}. \tag{15}$$

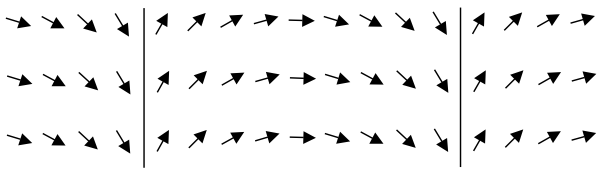

Figure 3. A striped defect lattice of alternating domains and domain walls in a two-dimensional film. Unlike the structure in figure 2, this pattern is favoured by chirality, because all the domains have the preferred chiral variation in the director. Adapted from reference [26].

From these results, we can draw several conclusions about the defect lattice. First, the defect lattice only exists when the chiral coefficient λ exceeds the defect line energy ϵ. This is reasonable, because the sequence of alternating domains and domain walls is only favoured in comparison with the uniform state if the system is 'sufficiently chiral', that is, if it gains more free energy from the modulation across a domain than it loses by introducing a domain wall. Increasing the chiral coefficient λ reduces the stripe width, because it favours the formation of more stripes. By contrast, increasing the defect line energy ϵ or the mean Frank constant $\bar{K}$ increases the stripe width. All three of these parameters may be functions of system variables, such as temperature. If changing temperature causes λ to pass through the value of ϵ, then the stripe width will diverge and the system will undergo a second-order transition from the striped phase to the uniform phase.

The striped phase is not the only type of defect lattice that can form in two-dimensional films of chiral liquid crystals. Another theoretical possibility, pointed out in reference [26], is the hexagonal lattice shown in figure 4. This lattice consists of hexagonal domains separated by domain walls. Each hexagonal domain has the favoured chiral variation of $\boldsymbol{c}$, and the domain walls allow this variation to be repeated periodically. There are topological vortices in $\boldsymbol{c}$ at the centres of the domains, and corresponding antivortices at the corners. The full phase diagram

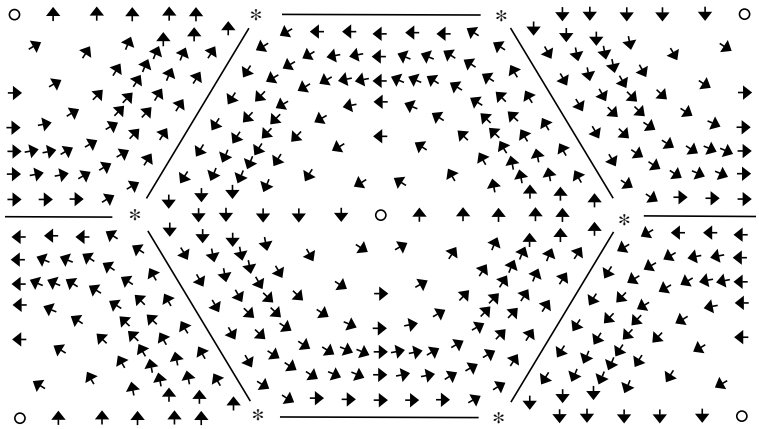

Figure 4. A hexagonal defect lattice of domains separated by domain walls. Each domain has the favoured chiral variation of the director. The structure has vortices at the centres of the domains and antivortices at the corners. Adapted from reference [26].

for the uniform phase, the striped phase, and the hexagonal lattice has not yet been worked out. However, we can say that the energy balance between the striped phase and the hexagonal lattice depends on two factors. First, the striped phase has a combination of bend and splay in $\boldsymbol{c}$, while the hexagonal lattice has more nearly pure bend. Hence, the hexagonal lattice is favoured in a system with $K_1 \gg K_3$. Second, the free energy of the hexagonal lattice includes a logarithmic interaction between vortices and antivortices, in addition to the terms discussed for the striped phase. Hence, the hexagonal lattice is favoured in highly chiral systems, in which the lattice spacing becomes small and this interaction becomes large and favourable. To the best of our knowledge, the hexagonal lattice has not yet been seen experimentally, which suggests that these conditions have not been achieved. It remains a theoretical possibility for future experiments.

3.3. More microscopic view of defect lines

In the previous section, we took a *macroscopic* point of view, in which the domains of the liquid-crystal film are described by continuum elastic theory and the domain walls are just defect lines. In this point of view, we neglect the internal structure of the domain walls, and just suppose that the domain walls have some energy ϵ per unit length. This wall energy is not predicted by the theory; rather, it is an input parameter for the theory.

It is possible to discuss the same lattice of domains and domain walls using a more *microscopic* point of view, in which the same theory describes both the domains and the domain walls. Such a microscopic theory is analogous to the theory for a cholesteric phase in a magnetic field presented in section 2, in which the free-energy functional was used both for the domains and for the solitons between the domains. The advantage of the more microscopic approach is that it gives a model for the internal structure of the domain walls, and makes a prediction for the domain wall energy. The disadvantage is that the microscopic theory is less general than the macroscopic theory—a different microscopic theory is needed for each type of domain wall.

One microscopic theory for the lattice of domains and domain walls was developed in references [26–28]. This theory supposes that the magnitude of the molecular tilt in the smectic-C phase is not fixed, but rather can vary as a function of position. The tilt magnitude

has a favoured value that it will assume in most of the film (the domains), but it can deviate from this favoured value in certain regions (the domain walls). To describe this variation mathematically, we allow the projection $\boldsymbol{c}(x, y)$ to vary in length as well as direction. The free energy then becomes

$$F = \int \mathrm{d}^2x \left[-\frac{1}{2}r|\boldsymbol{c}|^2 + \frac{1}{4}u|\boldsymbol{c}|^4 - \lambda|\boldsymbol{c}|^2\hat{\boldsymbol{z}}\cdot\boldsymbol{\nabla}\times\boldsymbol{c} + \frac{1}{2}K_1(\boldsymbol{\nabla}\cdot\boldsymbol{c})^2 + \frac{1}{2}K_3(\boldsymbol{\nabla}\times\boldsymbol{c})^2 \right]. \quad (16)$$

Here, the r- and u-terms are the standard Ginzburg–Landau expansion of the free energy in powers of $\boldsymbol{c}$. They favour the tilt magnitude $|\boldsymbol{c}| = \sqrt{r/u}$ in most of the film, but allow a different tilt magnitude in certain regions. The λ-term gives the favoured variation in the director due to molecular chirality. This term is written as $|\boldsymbol{c}|^2\hat{\boldsymbol{z}}\cdot\boldsymbol{\nabla}\times\boldsymbol{c}$ rather than just $\hat{\boldsymbol{z}}\cdot\boldsymbol{\nabla}\times\boldsymbol{c}$ because the latter term is a total derivative, which integrates to a constant depending only on the boundary conditions. By contrast, $|\boldsymbol{c}|^2\hat{\boldsymbol{z}}\cdot\boldsymbol{\nabla}\times\boldsymbol{c}$ is not a total derivative because the factor $|\boldsymbol{c}|^2$ couples variations in the magnitude of $\boldsymbol{c}$ with variations in the orientation.

The minimization of this free energy was worked out in references [26–28]. Those studies show explicitly that the optimum texture of $\boldsymbol{c}(x, y)$ breaks up into domains and domain walls. In the domains, the magnitude of $\boldsymbol{c}$ is approximately $\sqrt{r/u}$, and the orientation of $\boldsymbol{c}$ bends in the sense favoured by chirality. In the domain walls, the magnitude of $\boldsymbol{c}$ is greatly reduced, and the orientation bends back in the opposite sense. The system does not lose as much free energy from the reverse bend in the domain walls as it gains from the forward bend in the domains because of the coupling between variations in the magnitude of $\boldsymbol{c}$ with variations in the orientation. As in the macroscopic theory, the domains and domain walls can be arranged in stripes or in a hexagonal lattice.

An alternative microscopic theory has been developed specifically for *tilted hexatic* phases, which are known as smectic-I, smectic-F, and smectic-L [23] (see also related work [29, 30]). These phases have order in the orientation of the molecular tilt *and* order in the orientations of the intermolecular 'bonds' (not chemical bonds, but lines indicating the directions from one molecule to its nearest neighbours in the smectic layer). These two orientations are coupled by an interaction potential that favours a particular alignment of the molecular tilt with respect to the bond directions. The favoured alignment is along a nearest-neighbour bond direction in the smectic-I phase, halfway between two nearest-neighbour bonds in the smectic-F phase, or at an intermediate orientation in the smectic-L phase. In a tilted hexatic phase of *chiral* molecules, shown in figure 5, the molecular chirality causes the tilt direction to rotate across a domain, and the bond direction must rotate with it in order to keep the favoured alignment. In a domain wall, the tilt direction jumps by 60° from one bond direction to another, equivalent bond direction. Hence, the tilt and bond directions are locked

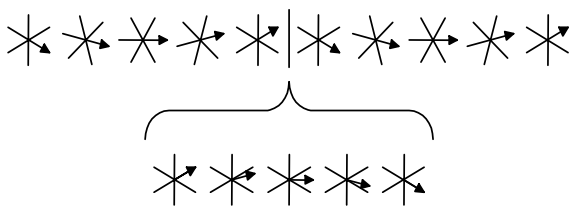

Figure 5. A striped defect lattice in a tilted hexatic (smectic-I) phase. The six-pointed stars represent the hexatic bond directions, and the arrows represent the tilt direction (i.e. the projection of the molecular director into the smectic layer plane). The top half of the figure shows that the tilt and bond directions rotate together across each domain. The bottom half shows that the tilt deviates from the favoured alignment with the bonds inside the narrow defect walls.

together everywhere in the domains, and only deviate from the favoured alignment in the domain walls. The line energy and width of the domain walls can both be calculated in terms of the tilt–bond interaction potential and the elastic constants [29,30]. Hence, this theory gives a specific model for the relationship between the tilt and bond directions in the domain walls, but it reduces to the same macroscopic theory as was studied earlier for the chiral texture of the domains.

The domain walls might have other internal structures that have not yet been considered in the literature. For example, in a two-component mixture of liquid crystals, the domains might have the optimal composition of the two components, while the domain walls would have a different composition. Equivalently, in a system with a single liquid-crystal component plus impurities, the domain walls might be regions where the impurities preferentially accumulate. All that is necessary is that the domain walls must have a *different* microscopic structure to the domains, and that the different microscopic structure must reduce the free-energy cost for short-length-scale variations in the tilt direction $\boldsymbol{c}$. Any such microscopic structure can give the macroscopic structure discussed in the previous section, with a periodic lattice of domains and domain walls.

3.4. Smectic-A phase under an electric field

The work discussed in sections 3.1–3.3 is concerned with two-dimensional films of liquid crystals in phases with spontaneous tilt order, i.e. the smectic-C or tilted hexatic phases. A recent paper has shown that related considerations apply to films of the untilted smectic-A phase of chiral molecules under an electric field [31]. In the absence of an electric field, the smectic-A phase does not have tilt order; the average molecular director is aligned along the smectic layer normal. This director alignment along the layer normal is unaffected by chirality (unless the chirality is so strong that it actually disrupts the smectic layer structure, as discussed in section 4 below). When an electric field is applied in the smectic layer plane, it induces a tilt of the director away from the layer normal. This induced tilt is called the electroclinic effect. The system then experiences a frustration analogous to the cholesteric phase in a magnetic field: the field favours a particular alignment of the induced tilt, while chirality favours a modulation in the tilt direction.

The smectic-A phase under an electric field has been modelled in reference [31] using the free energy

$$F = \int \mathrm{d}^2x \left[\frac{1}{2} r|\boldsymbol{c}|^2 + \frac{1}{4} u|\boldsymbol{c}|^4 + b\hat{\boldsymbol{z}} \cdot \boldsymbol{E} \times \boldsymbol{c} - \lambda|\boldsymbol{c}|^2 \hat{\boldsymbol{z}} \cdot \boldsymbol{\nabla} \times \boldsymbol{c} + \frac{1}{2} K_1 (\boldsymbol{\nabla} \cdot \boldsymbol{c})^2 + \frac{1}{2} K_3 (\boldsymbol{\nabla} \times \boldsymbol{c})^2 \right]. \tag{17}$$

This free energy is equivalent to equation (16) for the smectic-C phase, except that the coefficient of $|\boldsymbol{c}|^2$ is positive, indicating that the smectic-A phase does not have spontaneous tilt order, and a coupling of the tilt to the applied field $\boldsymbol{E}$ has been added. The question is whether the minimum of this free energy is a uniform tilt or a chiral modulation in $\boldsymbol{c}(x, y)$. This was investigated through a combination of continuum elastic theory and lattice simulations. The results showed that the state of uniform tilt can become unstable to the formation of chiral stripes, similar to the stripes seen in films of the smectic-C phase, which resolve the frustration between chirality and the applied field. The theoretical phase diagram, shown in figure 6, predicts that stripes will occur for a certain range of field. This range becomes larger as the chiral coefficient λ increases and as the system approaches the transition from smectic-A to smectic-C, where r passes through 0.

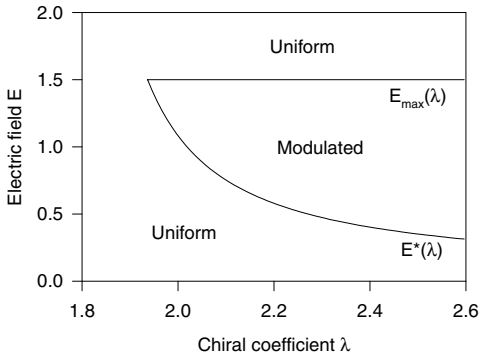

Figure 6. The phase diagram for a smectic-A film of chiral molecules under an applied electric field, showing the uniform state and the chiral modulation. The phase diagram is expressed in terms of the chiral coefficient λ and the applied field $\boldsymbol{E}$, for fixed parameters $r = 0.5$, $u = 1$, $b = 1$, and $\bar{K} = \frac{1}{2}(K_1 + K_3) = 1.5$. From reference [31].

In most electroclinic liquid crystals developed for device applications, this modulation has not been seen, suggesting that the chiral coefficient λ is not large enough to give stripes. However, certain electroclinic liquid crystals show an otherwise unexplained striped modulation that is consistent with this chiral mechanism [31–33]. Hence, controlling this effect may become important for optimizing liquid-crystal devices.

3.5. Chiral symmetry breaking

So far we have considered the effects of chirality on systems of fixed chirality. Some related effects can occur in systems that undergo a chiral symmetry-breaking transition, in which they spontaneously break reflection symmetry and select a handedness. Some possible mechanisms for such symmetry breaking were proposed in reference [34]. The first and simplest is just phase separation of a racemic mixture. If a mixture of opposite enantiomers separates into its chiral components, then any local region of the system is predominantly right- or left-handed. An appropriate chiral order parameter would then be the difference in densities of the two enantiomers. A second possibility, which can occur even in systems of pure achiral molecules, is that the molecules can pack in a two-dimensional film in two inequivalent ways that are mirror images of each other. The chiral order parameter would then be the difference of densities of the two types of packing. A third possibility is the formation of the tilted hexatic phase known as smectic-L, mentioned in section 3.3, which breaks reflection symmetry in the relationship between the tilt and bond directions.

If a two-dimensional liquid-crystal film undergoes a chiral symmetry-breaking transition, how does the spontaneous chirality affect the ordering of the film? This question has been addressed in references [34–36]; here we review the discussion in the first of those papers. The free energy can be written in the form

$$F = \int \mathrm{d}^2x \left[\frac{1}{2}\kappa(\boldsymbol{\nabla}\psi)^2 + \frac{1}{2}t\psi^2 + \frac{1}{4}u\psi^4 + \frac{1}{2}K_1(\boldsymbol{\nabla}\cdot\boldsymbol{c})^2 + \frac{1}{2}K_3(\boldsymbol{\nabla}\times\boldsymbol{c})^2 - \lambda\psi\boldsymbol{\nabla}\times\boldsymbol{c}\right]. \tag{18}$$

Here, $\psi(x, y)$ is the pseudoscalar order parameter representing the extent and handedness of chiral symmetry breaking, and $\boldsymbol{c}(x, y)$ is the projection of the molecular director into the layer plane. (This study assumes that the tilt is constant in magnitude; reference [35] allows it to

vary.) The first three terms in F are a Ginzburg–Landau expansion in powers of ψ, the next two terms are the Frank free energy for variations in $\boldsymbol{c}$, and the final term couples these variables. Note that $\boldsymbol{\nabla} \times \boldsymbol{c}$ is multiplied by a chiral order parameter which can itself vary across the film.

By minimizing the free energy over $\psi(x, y)$ and $\boldsymbol{c}(x, y)$, reference [34] obtained the phase diagram shown in figure 7. At high temperature, the system is in a uniform nonchiral phase. As the temperature decreases, the system undergoes a continuous chiral symmetry-breaking transition. Because the local order parameter $\psi(x, y)$ is nonzero, it favours a bend of the director, just as in the chiral films discussed in sections 3.1–3.4. In this case, however, since the system has spontaneous rather than fixed chirality, it has a different way to resolve the geometric frustration associated with chirality. Instead of introducing domain walls in which the director jumps back rapidly, this system can simply reverse the sign of $\psi(x, y)$, which favours a continuous backward bend of the director. Hence, the system breaks up into stripes of alternating right- and left-handed chirality, as shown in figure 8. At high temperature, the stripes involve a smooth, sinusoidal modulation of both ψ and $\boldsymbol{c}$. As the temperature decreases, this smooth modulation crosses over into a sharper modulation, with domains of approximately constant positive or negative ψ separated by domain walls. These domain walls, unlike the domain walls studied in systems of fixed chirality, are solitons in which ψ changes sign but $\boldsymbol{c}$ is continuous. (At high chirality, the system can also have a square lattice or 'checkerboard' phase, with alternating square cells of right- and left-handed chirality.) At low temperature, the spacing of the soliton walls diverges and the system has a transition into a phase of uniform chirality. This phase may or may not show the stripes studied in sections 3.2 and 3.3, with fixed ψ and solitons in $\boldsymbol{c}$, depending on the free-energy cost of such solitons.

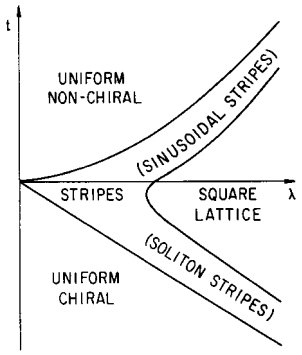

Figure 7. The mean-field phase diagram for chiral symmetry breaking in a two-dimensional film. The parameter t represents temperature, while λ is the coupling between the chiral order parameter ψ and the curl of the tilt director field $\boldsymbol{c}$. This phase diagram is a schematic view, not drawn to scale. From reference [34].

The clearest experimental demonstration of this effect has been in experiments on freely suspended liquid-crystal films [37]. These experiments show a transition from a uniform nonchiral phase to a striped phase, which has a spontaneous bend in $\boldsymbol{c}$. The sign of the bend $\boldsymbol{\nabla} \times \boldsymbol{c}$ alternates in successive stripes. The stripe width diverges at the phase transition, in at least qualitative agreement with the theoretical prediction.

3.6. Spiral defects

For the striped phases discussed in the previous sections, the lowest-energy state is to have straight, parallel stripes. However, thermal fluctuations can lead to curvature of the stripes.

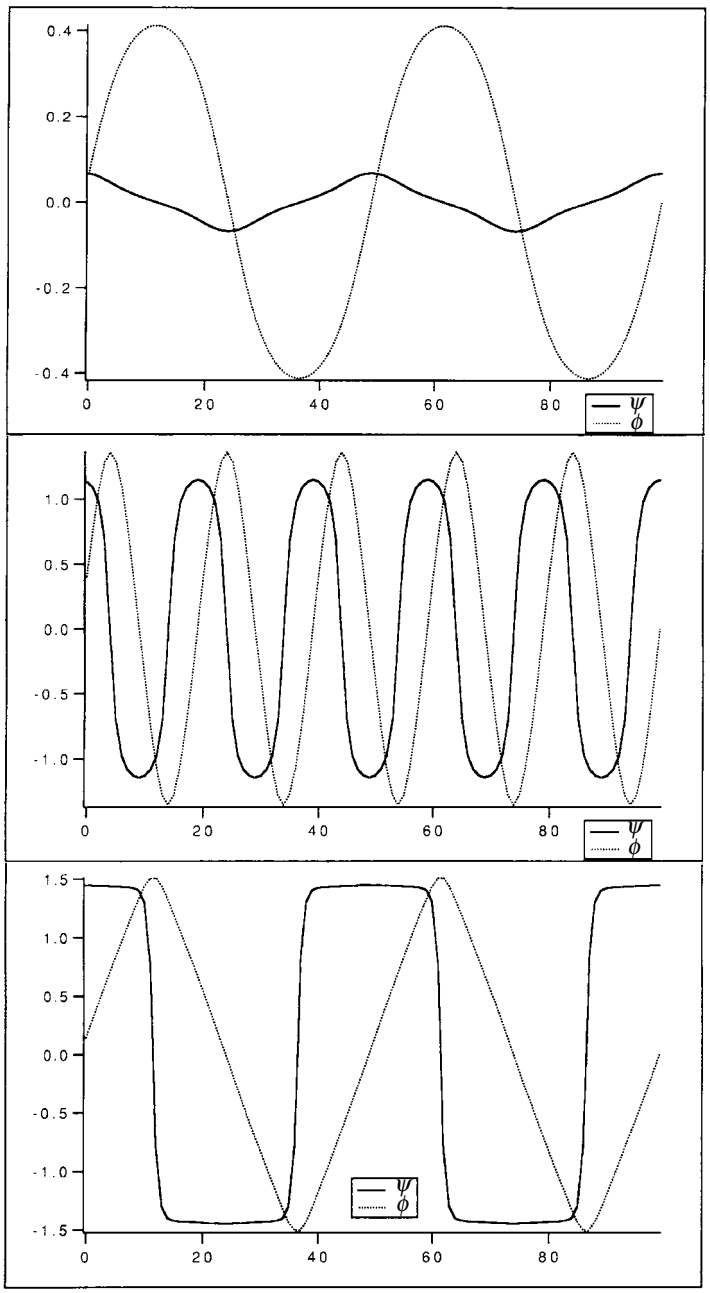

Figure 8. The modulation in the chiral order parameter $\psi(x)$ and the tilt director $\boldsymbol{c}(x) = (\cos\phi(x), \sin\phi(x))$ at three temperatures in the symmetry-breaking striped phase. Top: $t = 0.9$. Middle: $t = -1$. Bottom: $t = -2$. In all three plots, $\lambda = K_1 = K_3 = \kappa = u = 1$. Note the evolution from the sinusoidal-stripe regime at high temperature to the soliton-stripe regime at low temperature. From the second of references [34].

Moreover, *defects* in the striped phases can have an interesting spiral form, as shown in figure 9(a). Such spiral defects have been seen experimentally in freely suspended films

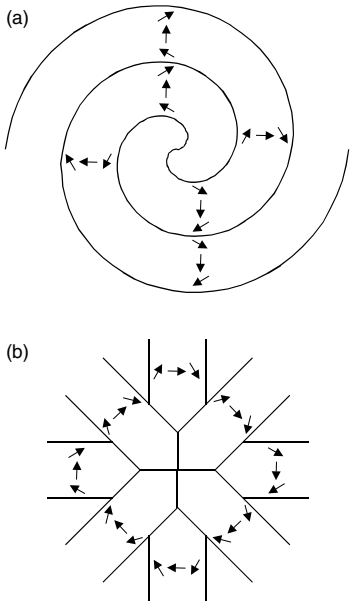

Figure 9. (a) A spiral defect resulting from the combination of a striped phase with a point vortex in the tilt director $\boldsymbol{c}$. (b) Dense branching morphology, an alternative structure for a point vortex in a striped phase. The spiral defect generally has a lower free energy than the dense branching morphology. Adapted from reference [40].

of chiral liquid crystals in tilted hexatic phases [23]. They have also been seen in Langmuir monolayers of achiral molecules [38, 39]—systems in which the stripes are driven by the up–down asymmetry rather than the chiral asymmetry, as discussed at the end of section 3.1.

The formation of spiral defects has been attributed to the following mechanism [40]. Suppose there is a point vortex in $\boldsymbol{c}$. A point vortex could arise from a localized impurity, from the kinetics of formation of the monolayer, from boundary conditions on a circular droplet, or from thermal fluctuations that nucleate a vortex–antivortex pair. Near the vortex core, there is more than the optimal bend. Away from the vortex core, the bend $\boldsymbol{\nabla} \times \boldsymbol{c}$ decreases as $1/r$, where r is the distance from the core. As a result, the defect generates domain walls, like the walls in the periodic striped pattern, and thereby increases the bend up to the optimal value. Further from the vortex core, the bend continues to decrease, or equivalently, the distance between the domain walls increases linearly with r. To maintain the optimal bend, the pattern of domain walls may buckle to form a right- or left-handed spiral, which maintains a constant spacing between walls, as in figure 9(a). Alternatively, the system may continue to generate more domain walls in a dense branching morphology, as shown in figure 9(b). Calculations have shown that the spiral has a lower free energy than the dense branching morphology for large system size, and hence it is the more common defect form.

Although it is tempting to associate the spiral form of the defect with the chirality of the molecules, one should note this mechanism depends only on the combination of a striped phase with a point vortex in $\boldsymbol{c}$. It can occur in films with an up–down asymmetry driving splay stripes, as well as in films with chirality driving bend stripes. The resulting spirals can be either right- or left-handed. Hence, the handedness of these defects can be regarded as a *macroscopic* chiral symmetry breaking on the length scale of the defect, in contrast with the microscopic chiral symmetry breaking discussed in the previous section.

3.7. Membrane curvature: ripples and tubules

In the discussion so far, we have seen how *flat* liquid-crystal films respond to the geometric frustration caused by chirality. But do the films need to remain flat? That depends on the type of film. Freely suspended films of thermotropic liquid crystals are generally stretched across an aperture, and hence are constrained by surface tension to remain nearly flat. Langmuir monolayers and Langmuir–Blodgett films also must remain nearly flat because they must conform to the shape of the substrate. However, lyotropic liquid crystals, consisting of lipid membranes separated by solvent, have much more freedom to curve out of the plane. For those systems, membrane curvature is another possible response to chirality.

Recent papers have considered chirality as a mechanism for inducing the $P_{\beta'}$ 'ripple' phases that are observed in lipid membranes [41–43]. These studies show that any modulation in the tilt director $\boldsymbol{c}$ will induce a modulation in the height of the membrane above a flat reference plane, thus giving a periodic ripple in the membrane curvature. Several distinct ripple phases with different symmetry are possible, depending on the orientation of $\boldsymbol{c}$ with respect to the ripple wavevector. Chirality is important for the structure of these phases because it leads to a coupling between tilt variations and curvature that is not present in nonchiral systems, and this coupling leads to asymmetric ripple shapes that are consistent with experimental results.

Lipid membranes are not limited to slight ripple distortions about a basically flat structure; they can also assume quite different shapes. As an important example, diacetylenic lipids form cylindrical tubules, with a typical diameter of 0.5 μm and a typical length of 10 μm to 1 mm [44]. These tubules have been studied extensively for use as templates for the formation of metal cylinders, for applications in electroactive composites and controlled-release systems. The formation of lipid tubules has been explained theoretically as a response to the chirality of the lipid molecules. A continuum elastic theory for flexible chiral membranes has shown that there is an intrinsic bending force on any chiral bilayer membrane with tilt order [45]. This early work has been extended in several ways by different investigators. In particular, references [46, 47] have shown that chirality has two simultaneous effects on a membrane: it induces the formation of a cylinder, with a radius that can be calculated in terms of the continuum elastic coefficients, and it induces the formation of stripes in the orientation of the molecular tilt on the cylinder. These stripes are equivalent to the stripes in flat films of chiral liquid crystals discussed in sections 3.2 and 3.3. They wind around the cylinder in a helical fashion, as shown in figure 10, and they should also induce slight ripples in the cylindrical curvature. Theoretical work on tubules and related lipid microstructures is reviewed and compared with experiments in a forthcoming publication [48].

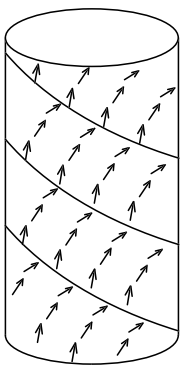

Figure 10. A striped pattern in the tilt director in the modulated state of a lipid tubule. The arrows indicate the direction of the molecular tilt, projected into the local tangent plane. From references [46, 47].

4. Defect structures in three dimensions

4.1. The twist-grain-boundary phase

In three dimensions, competing intrinsic interactions can lead to complex defect structures. A prototypical example of this is the twist-grain-boundary (TGB) phase of chiral, smectogenic liquid crystals, the analogue of the Abrikosov vortex lattice phase of type-II superconductors [49]. In this system, the periodic smectic order is incompatible with the helical cholesteric order favoured by the chiral molecules. As in two dimensions, we can either appeal to a more macroscopic picture in which defects allow for regions of twist and assume an energy penalty per unit length, or we can employ a microscopic picture which includes the relevant order parameter and correlation lengths to model the defect structure.

In this example we will use a microscopic picture, due to the (relative) simplicity of the chiral smectic-A phase. To model this system one introduces a complex order parameter ψ. The magnitude of ψ is a measure of smectic order, while the phase of ψ is associated with the spontaneously broken translational invariance of the layered smectic phase. The density of the material is simply $\rho(x) = \rho_0 + \mathrm{Re}\psi(x)$ where ρ_0 is the background density. In the smectic-A phase the layer normal is parallel to the local director $\hat{\boldsymbol{n}}$. When the molecules are chiral, the director undergoes fluctuations controlled by the free energy of equation (1) with magnetic field $\boldsymbol{H} = 0$. In the smectic phase we may write $\psi = |\psi| \exp\{\mathrm{i}q(z - u(x, y, z))\}$, where we have chosen the average layer normal to point along $\hat{\boldsymbol{n}}_0 = \hat{\boldsymbol{z}}$ and where $u(x, y, z)$ is the displacement field that describes fluctuations in the layered structure. To quadratic order in $\delta\hat{\boldsymbol{n}} = \hat{\boldsymbol{n}} - \hat{\boldsymbol{n}}_0$ and u, the free energy of this system is [2]

$$F = \frac{1}{2}\int \mathrm{d}^3x \, \{B(\partial_z u)^2 + \tilde{B}(\boldsymbol{\nabla}_\perp u - \delta\hat{\boldsymbol{n}})^2 + K_1(\boldsymbol{\nabla}_\perp \cdot \delta\hat{\boldsymbol{n}})^2 + K_2(\boldsymbol{\nabla}_\perp \times \delta\hat{\boldsymbol{n}} + q_0)^2 + K_3(\partial_z \, \delta\hat{\boldsymbol{n}})^2\} \tag{19}$$

where B and $\tilde{B}$ are elastic constants proportional to $|\psi|^2$ and $\boldsymbol{\nabla}_\perp \equiv \hat{\boldsymbol{x}}\,\partial_x + \hat{\boldsymbol{y}}\,\partial_y$ is the gradient in the xy-plane. The first term measures the relative compression of the smectic structure, while the second term is a measure of the misalignment of the nematic director with the local layer normal. The remaining three terms are the linearization of equation (1) in the absence of a magnetic field. This free energy, which is similar to the London free energy of a superconductor, is frustrated. The first and last terms in equation (19) vanish identically for z-independent solutions without affecting the remaining terms, and so the effective free energy is simply

$$F = \frac{1}{2}\int \mathrm{d}^3x \, \left\{\tilde{B}(\boldsymbol{\nabla}_\perp u - \delta\hat{\boldsymbol{n}})^2 + K_1(\boldsymbol{\nabla}_\perp \cdot \delta\hat{\boldsymbol{n}})^2 + K_2(\boldsymbol{\nabla}_\perp \times \delta\hat{\boldsymbol{n}} + q_0)^2\right\}. \tag{20}$$

Note that this free energy, which is the sum of three positive definite terms, can *never vanish*: if the first term in equation (20) vanishes, then $\boldsymbol{\nabla}_\perp u = \delta\hat{\boldsymbol{n}}$, so $\boldsymbol{\nabla}_\perp \times \delta\hat{\boldsymbol{n}} = \boldsymbol{\nabla}_\perp \times \boldsymbol{\nabla}_\perp u$ must vanish identically and the third term is nonzero. Conversely, if the third term vanishes then $\boldsymbol{\nabla}_\perp \times \delta\hat{\boldsymbol{n}} = -q_0$ and there is no nonsingular solution u that can make the first term vanish. Indeed, even if we force the second term to vanish so that $\boldsymbol{\nabla}_\perp \cdot \delta\hat{\boldsymbol{n}} = 0$, then $\delta\hat{\boldsymbol{n}} = q_0 y\hat{\boldsymbol{x}}$ and it is clear that the first term in equation (20) will diverge with system size so strongly that even the free-energy density will diverge. As in the case of the cholesteric in the magnetic field, however, we can identify two extreme solutions. As we have argued, if $\tilde{B}$ is nonzero then we must choose $\boldsymbol{\nabla}_\perp \times \delta\hat{\boldsymbol{n}} = 0$ for a finite energy density. The smectic phase thus completely expels twist. Another possibility, however, is to lose the smectic order: since $\tilde{B}$ is proportional to $|\psi|^2$ it is possible to destroy the smectic order and consequently have $\tilde{B}$ vanish. Then $\boldsymbol{\nabla}_\perp \times \delta\hat{\boldsymbol{n}} = -q_0$ and the cholesteric phase ensues.

Not surprisingly, just as in the example in section 2, it is possible to have a mixture of both effects. By letting $|\psi|$ vanish in isolated regions it is possible to relieve the intrinsic frustration in this system. Such a defect is a screw dislocation in which the layers are punctuated by a helicoid with the result that $u \propto \tan^{-1}(y/x)$. It is straightforward to check [2] that an extremum of equation (20) is

$$\begin{aligned} u &= \frac{md\phi}{2\pi} \\ \delta\hat{\boldsymbol{n}}_\phi &= \frac{md}{2\pi\rho} - \frac{md}{2\pi\lambda}\mathcal{K}_1(\rho/\lambda) \\ \delta\hat{\boldsymbol{n}}_\rho &= 0 \end{aligned} \tag{21}$$

where m is an integer, d is the smectic layer spacing, $\mathcal{K}_1(\cdot)$ is the modified Bessel function of order 1, $\rho = \sqrt{(x^2 + y^2)}$, $\phi = \tan^{-1}(y/x)$, and $\lambda \equiv \sqrt{(K_2/\tilde{B})}$ is the twist penetration depth. A measure of the defect's strength is its Burgers vector $b \equiv md$—an integer multiple of the layer spacing. While u is singular at the origin, $\delta\hat{\boldsymbol{n}}$ is well defined. However, in order for the free energy to remain finite, $\tilde{B}$ must vanish at the origin, and thus $|\psi| \to 0$ in a region of size ξ. To minimize the free energy we would substitute the above solution into equation (20) for arbitrary m. We would find that as q_0 increases from 0 the ground state would switch from the $m = 0$ solution to the $m = \pm 1$ solution. At this point the screw dislocations would proliferate.

While the physics of a single defect (as shown in figure 11) was well understood for many years [50], the full geometry resulting from a proliferation of defects was determined by Renn and Lubensky in 1988 [51]. It was discovered soon thereafter in the homologous series *S*-1-methy-heptyl4′-[(4″-*n*-alkyloxyphenyl)propionoyloxyl-biphenyl-4-carboxylate] (nP1M7) later that year [52]. Since the TGB phases exist over narrow temperature ranges, it is quite likely that they had been overlooked in prior studies—it is in this way that theoretical constructs serve as guideposts for experiment. The TGB phase is composed of a sequence of grain boundaries, separated by ℓ_b, with each of these boundaries being composed of screw dislocations ℓ_d apart, as shown in figure 12. To understand how a periodic array of screw dislocations effects a twist in the smectic layer normal, it is convenient to

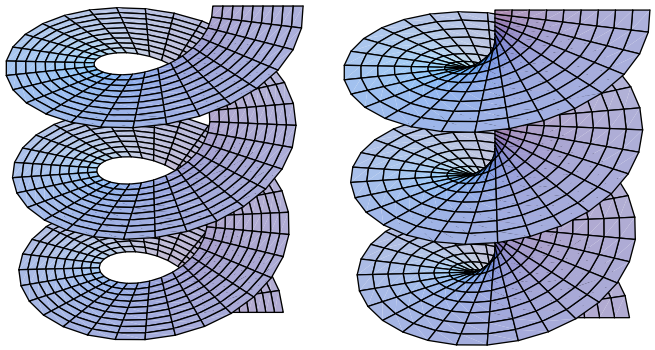

(a) ***(b)***

Figure 11. The structure of a single screw dislocation in a smectic-A phase. In (a) the core is shown, which is typically nematic. In (b) there is no hole, appropriate for a description which ignores the details of the core.

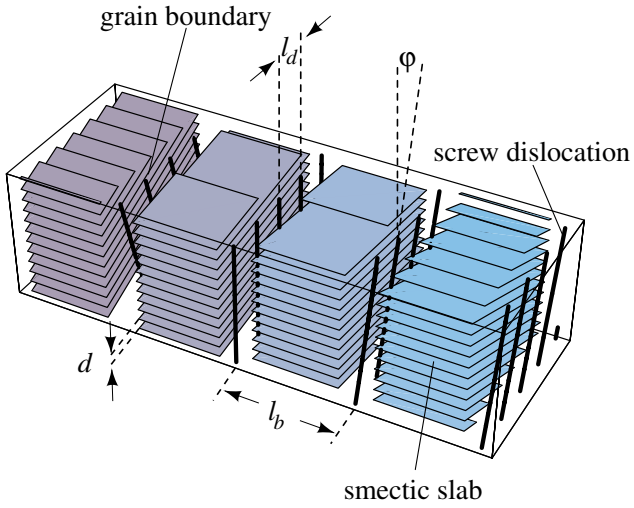

Figure 12. A twist-grain-boundary (TGB) phase, consisting of a smectic-A phase with a sequence of grain boundaries separated by a distance ℓ_b, with each of these grain boundaries composed of screw dislocations separated by a distance ℓ_d. Adapted from reference [51].

employ the Poisson summation formula to determine the strains $\partial_i u(x, y, z)$. In reference [53] it was found that, for screw dislocations parallel to the z-axis with Burgers vector b, separated by ℓ_d along the y-axis,

$$\begin{aligned}
\partial_x u &= -\frac{b}{2\ell_d}\frac{\sin(2\pi y/\ell_d)}{\cosh(2\pi x/\ell_d) - \cos(2\pi y/\ell_d)} \\
\partial_y u &= \frac{b}{2\ell_d}\frac{\sinh(2\pi x/\ell_d)}{\cosh(2\pi x/\ell_d) - \cos(2\pi y/\ell_d)} \\
\partial_z u &= 1 - \sqrt{1 - (b/2\ell_d)^2}.
\end{aligned} \tag{22}$$

By comparing the layer normals $\boldsymbol{N} = [\partial_x u, \partial_y u, \partial_z u - 1]/\sqrt{1 - 2\,\partial_z u + (\boldsymbol{\nabla} u)^2}$ at $x = \pm\infty$, one can check that the array of defects rotates the smectic structure by an angle $\alpha = 2\sin^{-1}(b/2\ell_d)$. The TGB phase is an assembly of such grain boundaries. Recent progress has been made on calculating the geometry of the quiescent state of the TGB phase—the ratio ℓ_b/ℓ_d is relatively constant over a range of parameters and is approximately 0.94 [54]. This is both qualitatively and quantitatively in very close agreement with the experiments of Navailles and co-workers [55].

4.2. Chiral lyotropic phases

Since the TGB phase is a defect phase of a layered system, it is natural to ask whether a single lamella might tear to form the analogue of screw dislocation [56]. Unlike the screw dislocation in a smectic, however, the core of the defect is not nematic but is filled with solvent. Thus, unlike the case for the systems that we have discussed so far, the core size is not set by parameters in a Landau theory but by the balance between elasticity and the line tension of an exposed edge. Although reminiscent of the tubule phases described in section 3.7, these helicoidal structures are different in detail. Recall that for a surface we may define two invariant measures of curvature: the mean curvature is the average of the two principal curvatures while the Gaussian curvature is the product. In tubules the mean curvature couples

to the chirality, while in the helicoids the mean curvature vanishes. Moreover, when integrated over a closed surface the Gaussian curvature yields a topological constant and is thus often neglected. However, because the helicoid is formed by tearing the plane, the total Gaussian curvature can change. This effect may play a role in promoting and stabilizing the newly discovered smectic blue phases [57, 58] as well.

4.3. The moiré phase

While the smectic liquid crystal represents one-dimensional translational order, the hexagonal columnar phase is an example of two-dimensional translational order in the plane perpendicular to the local director $\hat{\boldsymbol{n}}$. It can be thought of as stacks of discs arranged in a hexagonal lattice. However, in each stack there is no translational order—the discs form one-dimensional liquids. An elasticity theory can be developed for this phase [59] based on the principles of broken symmetry. Within this theory, the defect line tension may be calculated and one finds that screw dislocations, as depicted in figure 13, have a finite energy per unit length. We will take a more macroscopic approach to discussing these defect phases, using only the finiteness of the line tension from the more microscopic theory.

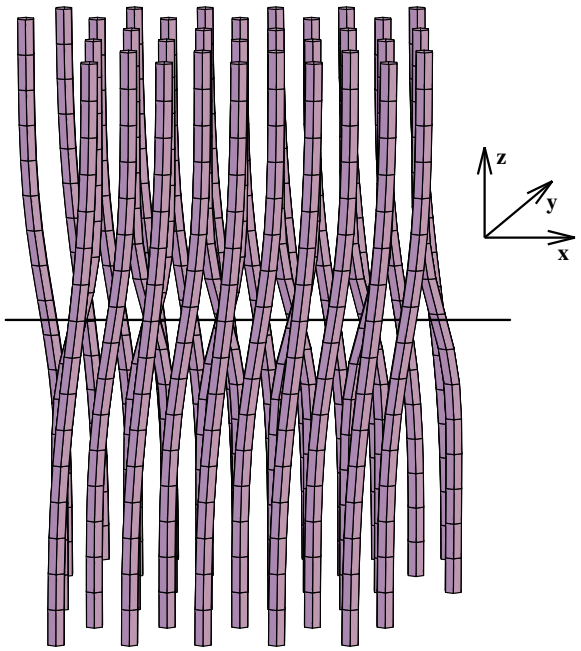

Figure 13. The structure of a single screw dislocation in a hexagonal columnar phase. From reference [59].

Because the columnar crystal has two displacement or phonon modes, it is possible to have more than one type of defect phase. Two have been proposed, although other defect complexions may be possible. The first is a close analogue of the smectic TGB phase: the polymer tilt-grain-boundary phase. In this phase, regions of undistorted hexagonal columnar crystal are separated by grain boundaries which effect a twist of the local nematic director. As in the TGB phase, the cholesteric rotation is broken into discrete jumps. The single grain boundaries are each composed of an array of parallel screw dislocations. Again, the combined effect of these defects may be calculated [59], and they lead to a twisting of the columnar phase.

A different defect phase is also possible: the moiré phase. This phase is, in some sense, a three-dimensional analogue of the hexagonal domain phase described in section 3.2. Here, however, the defect lattice rotates the intermolecular bonds, twisting the crystal along the director axis as shown in figure 14. This phase can be thought of as a stack of hexagonal crystals, each successive one rotated by a special angle to produce a 'moiré' pattern. Recent experiments on nucleosome core particles [60] may exhibit this exotic phase.

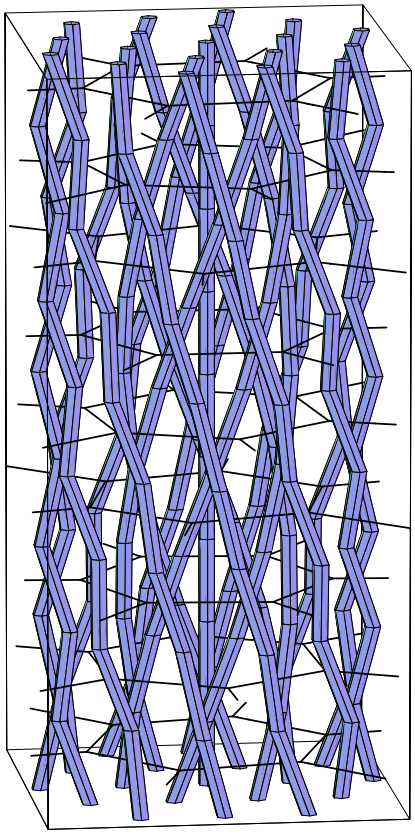

Figure 14. A moiré phase, composed of a lattice of screw dislocations in a hexagonal columnar phase. From reference [59].

Acknowledgments

RDK was supported by NSF CAREER Grant DMR97-32963 and the Alfred P Sloan Foundation. JVS was supported by the Naval Research Laboratory and the Office of Naval Research.

References

[1] For the original work on the Ising antiferromagnet on a triangular lattice, see
Wannier G H 1950 *Phys. Rev.* **79** 357
and for a recent study, see
Chakraborty B, Gu L and Yin H 2000 *J. Phys.: Condens. Matter* **12** 6487

[2] Chaikin P M and Lubensky T C 1995 *Principles of Condensed Matter Physics* (Cambridge: Cambridge University Press) section 9.6
[3] Pasteur L 1848 *Ann. Chim. Phys. Ser. 3* **24** 442
[4] Harris A B, Kamien R D and Lubensky T C 1997 *Phys. Rev. Lett.* **78** 1476
Harris A B, Kamien R D and Lubensky T C 1997 *Phys. Rev. Lett.* **78** 2867 (erratum)
[5] Harris A B, Kamien R D and Lubensky T C 1999 *Rev. Mod. Phys.* **71** 1745
[6] Raimondi M E and Seddon J M 1999 *Liq. Cryst.* **26** 305
[7] Imhof A and Pine D J 1997 *Nature* **389** 948
[8] Park M, Harrison C, Chaikin P M, Register R A and Adamson D H 1997 *Science* **276** 1401
[9] Meyer R B 1968 *Appl. Phys. Lett.* **12** 281
Meyer R B 1969 *Appl. Phys. Lett.* **14** 208
[10] Frank F C 1958 *Discuss. Faraday Soc.* **25** 19
[11] See, for instance,
Pokrovsky V L and Talapov A L 1984 *Theory of Incommensurate Crystals* translated by J G Adashko (New York: Harwood Academic)
[12] See, for instance,
de Gennes P G and Prost J 1993 *The Physics of Liquid Crystals* 2nd edn (Oxford: Oxford University Press) section 6.2.2.3
[13] Bogomol'nyi E B 1976 *Yad. Fiz.* **24** 861 (Engl. Transl. 1976 *Sov. J. Nucl. Phys.* **24** 449)
[14] Mermin N D 1979 *Rev. Mod. Phys.* **51** 591
[15] Kamien R D and Levine A J 2000 *Phys. Rev. Lett.* **84** 3109
[16] Strey H H, Wang J, Podgornik R, Rupprecht A, Yu L, Parsegian V A and Sirota E B 2000 *Phys. Rev. Lett.* **84** 3105
[17] Spector M S, Prasad S K, Weslowski B T, Kamien R D, Selinger J V, Ratna B R and Shashidhar R 2000 *Phys. Rev.* E **61** 3977
[18] Kralj S and Žumer S 1995 *Phys. Rev.* E **51** 366
Ambrožič M and Žumer S 1996 *Phys. Rev.* E **54** 5187
[19] Kamien R D and Powers T R 1997 *Liq. Cryst.* **23** 213
[20] Poulin P, Stark H, Lubensky T C and Weitz D A 1997 *Science* **275** 1770
[21] Meyer R B and Pershan P S 1973 *Solid State Commun.* **13** 989
[22] Clark N A, Van Winkle D H and Muzny C, unpublished (cited in reference [25])
[23] Dierker S B, Pindak R and Meyer R B 1986 *Phys. Rev. Lett.* **56** 1819
[24] Gorecka E, Glogarová M, Lejček L and Sverenyák H 1995 *Phys. Rev. Lett.* **75** 4047
[25] Langer S A and Sethna J P 1986 *Phys. Rev.* A **34** 5035
[26] Hinshaw G A, Petschek R G and Pelcovits R A 1988 *Phys. Rev. Lett.* **60** 1864
[27] Hinshaw G A and Petschek R G 1989 *Phys. Rev.* A **39** 5914
[28] Jacobs A E, Goldner G and Mukamel D 1992 *Phys. Rev.* A **45** 5783
[29] Selinger J V and Nelson D R 1989 *Phys. Rev.* A **39** 3135
[30] Selinger J V 1992 *Complex Fluids* ed E B Sirota, D Weitz, T Witten and J Israelachvili (Pittsburgh, PA: Materials Research Society) p 29
[31] Selinger J V, Xu J, Selinger R L B, Ratna B R and Shashidhar R 2000 *Phys. Rev.* E **62** 666
[32] Bartoli F J, Lindle J R, Flom S R, Shashidhar R, Rubin G, Selinger J V and Ratna B R 1998 *Phys. Rev.* E **58** 5990
[33] Sprunt S 2001 to be published
[34] Selinger J V, Wang Z-G, Bruinsma R F and Knobler C M 1993 *Phys. Rev. Lett.* **70** 1139
Selinger J V, Wang Z-G and Bruinsma R F 1993 *Biomolecular Materials* ed S T Case, J H Waite and C Viney (Pittsburgh, PA: Materials Research Society) p 235
[35] Ohyama T, Jacobs A E and Mukamel D 1996 *Phys. Rev.* E **53** 2595
[36] Zhao W, Wu C-X and Iwamoto M 2000 *Phys. Rev.* E **61** 6669
[37] Pang K and Clark N A 1994 *Phys. Rev. Lett.* **67** 703
[38] Ruiz-Garcia J, Qiu X, Tsao M-W, Marshall G, Knobler C M, Overbeck G A and Möbius D 1993 *J. Phys. Chem.* **97** 6955
[39] Usol'tseva N, Praefcke K and Blunk D 1998 *SPIE Proc.* **3319** 319
[40] Selinger J V and Selinger R L B 1995 *Phys. Rev.* E **51** R860
This paper is concerned with splay stripes induced by the up–down asymmetry of Langmuir monolayers; here we apply its results to bend stripes induced by chirality.
[41] Lubensky T C and MacKintosh F C 1993 *Phys. Rev. Lett.* **71** 1565
[42] Chen C M, Lubensky T C and MacKintosh F C 1995 *Phys. Rev.* E **51** 504

[43] Chen C M and MacKintosh F C 1996 *Phys. Rev.* E **53** 4933
[44] For a review of basic and applied research on lipid tubules, see
Schnur J M 1993 *Science* **262** 1669
[45] Helfrich W and Prost J 1988 *Phys. Rev.* A **38** 3065
[46] Selinger J V and Schnur J M 1993 *Phys. Rev. Lett.* **71** 4091
[47] Selinger J V, MacKintosh F C and Schnur J M 1996 *Phys. Rev.* E **53** 3804
[48] Selinger J V, Spector M S and Schnur J M 2001 to be published
[49] Lubensky T C 1995 *Physica* A **220** 99
[50] de Gennes P G 1973 *Solid State Commun.* **14** 997
[51] Renn S R and Lubensky T C 1988 *Phys. Rev.* A **38** 2132
Renn S R and Lubensky T C 1990 *Phys. Rev.* A **41** 4392
[52] Goodby J, Waugh M A, Stein S M, Pindak R and Patel J S 1989 *Nature* **337** 449
Goodby J, Waugh M A, Stein S M, Pindak R and Patel J S 1989 *J. Am. Chem. Soc.* **111** 8119
Strajer G, Pindak R, Waugh M A, Goodby J W and Patel J S 1990 *Phys. Rev. Lett.* **64** 13
Ihn K J, Zasadzinski J A N, Pindak R, Slanet A J and Goodby J 1992 *Science* **258** 275
[53] Kamien R D and Lubensky T C 1999 *Phys. Rev. Lett.* **82** 2892
[54] Bluvshtein I, Kamien R D and Lubensky T C 2001 in preparation
[55] Navailles L, Pansu B, Gorre-Talini L and Nguyen H T 1988 *Phys. Rev. Lett.* **81** 4168
[56] Kamien R D and Lubensky T C 1997 *J. Physique* II **7** 157
[57] Pansu B, Li M H and Nguyen H T 1997 *J. Physique* II **7** 751
Pansu B, Li M H and Nguyen H T 1998 *Eur. Phys. J.* B **2** 143
Pansu B, Grelet E, Li M H and Nguyen H T 2000 *Phys. Rev.* E **62** 658
[58] Kamien R D 1997 *J. Physique* II **7** 743
[59] Kamien R D and Nelson D R 1995 *Phys. Rev. Lett.* **74** 2499
Kamien R D and Nelson D R 1996 *Phys. Rev.* E **53** 650
[60] Livolant F and Leforestier A 2000 *Biophys. J.* **78** 2716
and see also
Fraden S and Kamien R D 2000 *Biophys. J.* **78** 2189